

## The Partial Replications of the Central Composite Designs for Spherical Regions

<sup>1</sup>Onyishi, Linus Ifeanyi <sup>2</sup>F.C. Eze

<sup>1</sup>Department of Mathematics and Statistics, Federal Polytechnic, Nasarawa, Nasarawa State, Nigeria

<sup>2</sup>Department of Statistics, Nnamdi-Azikiwe University, Awka, Nigeria

### Abstract:

Effects of partial replications of the star portion of the Central Composite Design (CCD) on the alternative axial distances were evaluated by comparing the performances of the replicated variations of the CCD in the spherical regions. The fractions of design space graphs (FDSG) of the star-replicated CCDs in the spherical region were plotted as well as the variance dispersion graph (VDG). The replication of the star portion of the CCD improved the prediction variance characteristics of the variations of the CCD in the spherical design regions.

**Keywords:** Central Composite Design; Star points; Axial Distances; Fraction Design Space Graph.

### 1 Introduction

The concept of replication of factorial components of the designs other than the centre point of the design was first introduced by Dykstra (1959). He argued that the measure of error obtained in factorial experiments in which each factor combination is run once does not provide true estimate of the experimental error in estimating the factor effects since the measure of the experimental error is obtained from the scatter among resulting measurements from design samples. This measure of experimental error, he considered to be the same as having repeated measures on one sample. Therefore, Dykstra (1959) proposed changing the experimental conditions after each run in order to obtain real duplicates that will provide true estimate of the experimental error even though this may incur higher number of experimental runs and cost of experimentation.

The idea of replicating factorial designs was extended to the replication of the cube and star portions of the central composite designs by Dykstra (1960). He argued that replicating only at the centre could be misleading since there is no assurance that the experimental error will be constant throughout the entire design region. He pointed out that variability might increase away from the centre of the design such that the estimate of the experimental error may be too small for proper evaluation of the coefficients of the second-order models. The cube and star portions of the CCD were examined for partial replication and suggestions made on possible advantages of replicating these portions of the CCD.

Draper (1982) examined the appropriate number of centre points that offers minimum prediction variance for central composite and Box-Behnken designs. To achieve this, he considered three variations of the CCD, namely: (i) one cube plus two stars, (ii) one cube plus one star and (iii) two cubes plus one star, for  $k = 5, 6, 7$  and  $8$  factors. The designs are evaluated by varying the number of centre points to know the design option that minimizes the integrated variance function proposed by Draper in the study.

Focus on improving prediction variance characteristics of the central composite design through the replication of cube and star portions of the design was recommended by Giovannitti-Jensen and Myers (1989). The variance dispersion graph developed by Giovannitti-Jensen and Myers (1989) for evaluating the prediction variances of response surface designs was extended to the central composite design with star replications by Borkowski (1995). The procedure adopted by Borkowski (1995) for the variance dispersion graph involved the development of analytical procedure as opposed to the Fortran-based programme used by Giovannitti-Jensen and Myers (1989) which becomes almost impossible to use for higher number of factors.

Borkowski (1995) approach has been adopted since its introduction as easier and more reliable approach for plotting variance dispersion graphs of the central composite designs. Chigbu et al. (2009) and Ukaegbu and Chigbu (2015a, 2015b) are some of the authors that have utilized the approach in plotting variance dispersion graphs for the evaluation of the central composite designs in both the spherical and cuboidal design regions. The same approach has been extended to the evaluation of prediction variance properties of split-plot central composite designs by Wesley et al. (2009).

Works by Chigbu and Ohaegbulem (2011) and Ukaegbu (2017) involved the evaluation and comparisons of the partially replicated variations of the central composite designs using single value criteria like the D- and G- criteria. In general, their works have shown that replicating the cube and star portions of the central composite designs does not improve the values of the D- and G-efficiencies of the design. Therefore, in this work, attention was paid mainly on the evaluation of the prediction variance characteristics of the central composite designs using the variance dispersion graphs and fraction of design space graphs when only the star portion is replicated.

Onyishi and Eze (2020) studied three axial distances as alternatives to the existing axial distances of the Central Composite Design (CCD) in spherical design regions with the aim of providing formidable alternatives to the existing axial distances of the CCD whose prediction properties are less extreme and more stable in the cuboidal design regions. The three alternative axial distances, namely the arithmetic, harmonic and geometric axial distances for spherical regions, were developed algebraically based on the concepts of the three Pythagorean means. The strengths and weaknesses of the alternative axial distances were validated by comparing their performances with the existing axial distances in the spherical regions. They used D- and G-efficiencies criteria for comparison. Their results show that spherical region in the three alternative axial distances are consistently better in terms of the D- and G-efficiencies.

## 2 Methodology

### 2.1 Axial Distance

The axial distance is developed using the three classical Pythagorean means namely the arithmetic mean, harmonic mean and geometric means.

The arithmetic mean is given by

$$A = \frac{1}{n} \sum_{i=1}^n a_i = n^{-1} \sum_{i=1}^n a_i \quad (1)$$

where  $a_i$  are set of data

The harmonic mean is also given by

$$H = \frac{n}{\frac{1}{x_1} + \frac{1}{x_2} + \dots + \frac{1}{x_n}} = \frac{n}{\sum_{i=1}^n \frac{1}{x_i}} = \left( \frac{\sum_{i=1}^n x_i^{-1}}{n} \right)^{-1} \quad (2)$$

where  $x_1, x_2, \dots, x_n$  are sets of observations.

The geometric means is given by

$$\left( \prod_{i=1}^n a_i \right)^{\frac{1}{n}} = \sqrt[n]{a_1 a_2 \dots a_n} \quad (3)$$

where  $a_i$  are set of data

### 2.2 Rotatable Axial Distance

Dykstra (1960) gave the value of the rotatable axial distance with cube and star replications,  $n_1$  and  $n_2$ , respectively as

$$a_R = \sqrt[4]{\frac{n_1 f}{n_2}} \quad (4)$$

With the replication of the star only, the rotatable axial distance becomes

$$a_R = \sqrt[4]{\frac{f}{n_2}} \tag{5}$$

This axial distance,  $a_R = \sqrt[4]{\frac{f}{n_2}}$ , will be used to develop another set of arithmetic, harmonic and geometric axial distances that accommodate the replication of the star portions of the central composite designs (CCD).

The new sets of axial distances for the spherical region are presented below.

For the arithmetic axial distance,

$$\alpha_{AS} = \frac{1}{s} \left\{ k^{1/2} + k^{1/4} + \left[ \frac{2^{k-q}}{n_2} \right]^{1/4} \right\}, s = 3, q > 0. \tag{6}$$

For the harmonic axial distance,

$$\alpha_{HS} = s \left\{ k^{-1/2} + k^{-1/4} + \left[ \frac{2^{-(k-q)/4}}{n_2^{1/4}} \right] \right\}^{-1}, s = 3, q > 0. \tag{7}$$

For the geometric axial distance,

$$\begin{aligned} \alpha_{GS} &= \left\{ k^{\frac{3}{4}} \times \frac{1}{n_2} \left( 2^{\frac{k-q}{4}} \right) \right\}^{\frac{1}{4}} \\ &= \left\{ \frac{k^3 2^{k-q}}{n_2} \right\}^{\frac{1}{4s}}. \end{aligned} \tag{8}$$

### 2.3 Prediction Variance

The prediction variance is given by

$$\text{var}[y(x)] = \sigma^2 x'^m (X'X)^{-1} x^m \tag{9}$$

where,

$(X'X)$  and  $(X'X)^{-1}$  are information matrix and its inverse respectively.

The Scaled Prediction Variance (SPV) of equation (9) is

$$\frac{N \text{var } y(x)}{\sigma^2} = Nx'^m (X'X)^{-1} x^m \tag{10}$$

The unknown parameter  $(\sigma^2)$  makes it difficult to use equation (10). Onukogu 1997 assume  $\sigma^2 = 1$ . This is to eliminate the unknown parameter.

In equation (10)  $N$  is the cost of experimentation for larger designs which is scaled. However must experimenter prefer to use unscaled prediction variance given by

$$\frac{\text{var}[y(x)]}{\sigma^2} = x'^m (X'X)^{-1} x^m \tag{11}$$

where  $\mathbf{x}^m = (\mathbf{1}, x_1, \dots, x_k; x_1^2, \dots, x_k^2; x_1x_2, \dots, x_{k-1}x_k)$  is the vector of design points in the design space.  $x_1, x_2, \dots, x_k$  are the linear model,  $x_1^2, x_2^2, \dots, x_k^2$  are the quadratic model and  $x_1x_2, \dots, x_{k-1}x_k$  are the mixed components of the model.

### 2.4 Graphical Comparison

The variance dispersion graphs (VDG) and fraction of design space graphs (FDSG) were used in comparing the alternative axial distances for the central composite designs with the existing axial distances in the spherical regions. As earlier pointed out, single point criteria like the D- and G-efficiencies cannot completely reflect the performances of a design throughout the entire design region. The graphical methods possess this unique quality and could reveal points of strengths and weaknesses of the competing designs within the design region by displaying the designs performances throughout the design space (Li et al, 2009 and Chigbu et al, 2009). The variance dispersion graphs (VDG) assess the prediction variance properties of the designs under study by displaying their scaled prediction variance performances at every point radius in the design space. A design with low and stable scaled prediction variances at every point radius is preferred. The fractions of design space graphs (FDSG) assess the prediction variance characteristics of competing designs by displaying the scaled prediction variances of the designs per volume of the design space (Ozol-Godfrey et al, 2005). Therefore, a design with small and stable scaled prediction variance at every fraction of the design space is preferred. The term 'stability' refers to a design maintaining small prediction variance over substantial portion of the design space or the entire design region. The variance dispersion graphs were plotted in MATLAB software package (Version 2014a) with the aid of computer programs developed in this work. The fraction of design space graphs were plotted in MATLAB software package (Version 2014a) after the fractions of design space and corresponding scaled prediction variance have been computed in Design Expert software package, Version 11. Three centre points were considered for each design for all the  $k$  factors under consideration.

### 3 Results and Discussions

The catalogue of values for the arithmetic, harmonic and geometric axial distances in the spherical region when the star point is replicated for  $k = 2$  to 10 factors are presented in Tables 1 and 2, respectively for  $n_2 = 2$  and 3.

**TABLE 1: Catalogue of Alpha Values for the Spherical Region with  $n_2 = 2$**

$K$	$f$	$2n_2k$	$\alpha_S$	$\alpha_P$	$\alpha_R$	$\alpha_{AS}$	$\alpha_{HS}$	$\alpha_{GS}$
2	$2^2$	8	1.4142	1.1892	1.1892	1.2642	1.2558	1.2599
3	$2^3$	12	1.7321	1.3161	1.4142	1.4874	1.4675	1.4772
4	$2^4$	16	2.0000	1.4142	1.6818	1.6987	1.6651	1.6818
5	$2^5$	20	2.2361	1.4954	2.0000	1.9105	1.8565	1.8840
6	$2^6$	24	2.4495	1.5651	2.3784	2.1300	2.0441	2.0891
7	$2^{6-1}$	24	2.4495	1.5651	2.0000	2.0049	1.9390	1.9719
8	$2^7$	28	2.6458	1.6266	2.8284	2.3699	2.2283	2.3003
9	$2^{7-1}$	28	2.6458	1.6266	2.3784	2.2169	2.1228	2.1712
10	$2^{7-2}$	28	2.6458	1.6266	2.0000	2.0908	2.0097	2.0494
	$2^8$	32	2.8284	1.6818	3.3636	2.6246	2.4088	2.5198
	$2^{8-1}$	32	2.8284	1.6818	2.8284	2.4462	2.3047	2.3784
	$2^{8-2}$	32	2.8284	1.6818	2.3784	2.2962	2.1920	2.2449
	$2^9$	36	3.0000	1.7321	4.0000	2.9107	2.5847	2.7496



	$2^{9-1}$	36	3.0000	1.7321	3.3636	2.6986	2.4835	2.5951
	$2^{9-2}$	36	3.0000	1.7321	2.8284	2.5202	2.3730	2.4495
	$2^{10}$	40	3.1623	1.7783	4.7568	3.2325	2.7553	2.9907
	$2^{10-1}$	40	3.1623	1.7783	4.0000	2.9802	2.6582	2.8228
	$2^{10-2}$	40	3.1623	1.7783	3.3636	2.7681	2.5513	2.6644
	$2^{10-3}$	40	3.1623	1.7783	2.8284	2.5897	2.4348	2.5149

**TABLE 2: Catalogue of Alpha Values for the Spherical Region with  $n_2 = 3$**

<b>K</b>	<b>f</b>	$2n_2k$	$\alpha_S$	$\alpha_P$	$\alpha_R$	$\alpha_{AS}$	$\alpha_{HS}$	$\alpha_{GS}$
2	$2^2$	12	1.4142	1.1892	1.0746	1.2260	1.2104	1.2181
3	$2^3$	18	1.7321	1.3161	1.2779	1.4420	1.4153	1.4282
4	$2^4$	24	2.0000	1.4142	1.5197	1.6446	1.6085	1.6259
5	$2^5$	30	2.2361	1.4954	1.8072	1.8462	1.7972	1.8214
6	$2^6$	36	2.4495	1.5651	2.1491	2.0546	1.9835	2.0197
7	$2^{6-1}$	36	2.4495	1.5651	1.8072	1.9406	1.8744	1.9064
8	$2^7$	42	2.6458	1.6266	2.5558	2.2760	2.1676	2.2239
9	$2^{7-1}$	42	2.6458	1.6266	2.1491	2.1405	2.0575	2.0991
10	$2^{7-2}$	42	2.6458	1.6266	1.8072	2.0265	1.9404	1.9813
	$2^8$	48	2.8284	1.6818	3.0393	2.5165	2.3489	2.4361
	$2^{8-1}$	48	2.8284	1.6818	2.5558	2.3553	2.2398	2.2994
	$2^{8-2}$	48	2.8284	1.6818	2.1491	2.2198	2.1224	2.1703
	$2^9$	54	3.0000	1.7321	3.6144	2.7822	2.5266	2.6581
	$2^{9-1}$	54	3.0000	1.7321	3.0393	2.5905	2.4199	2.5089
	$2^{9-2}$	54	3.0000	1.7321	2.5558	2.4293	2.3042	2.3681
	$2^{10}$	60	3.1623	1.7783	4.2983	3.0796	2.6997	2.8913
	$2^{10-1}$	60	3.1623	1.7783	3.6144	2.8517	2.5969	2.7291
	$2^{10-2}$	60	3.1623	1.7783	3.0393	2.6600	2.4843	2.5759
	$2^{10-3}$	60	3.1623	1.7783	2.5558	2.4988	2.3625	2.4313

It could be observed from comparing the values in Tables 1 and 2 that replicating the star portion of the central composite design reduces the rotatable, arithmetic, harmonic and geometric axial distances for the spherical region. The consequences of the reduction of the axial distances will now be measured on the prediction variance characteristics of the star-replicated central composite designs. The variance dispersion graphs and fraction of design space graphs of the star-replicated CCD are presented henceforth.

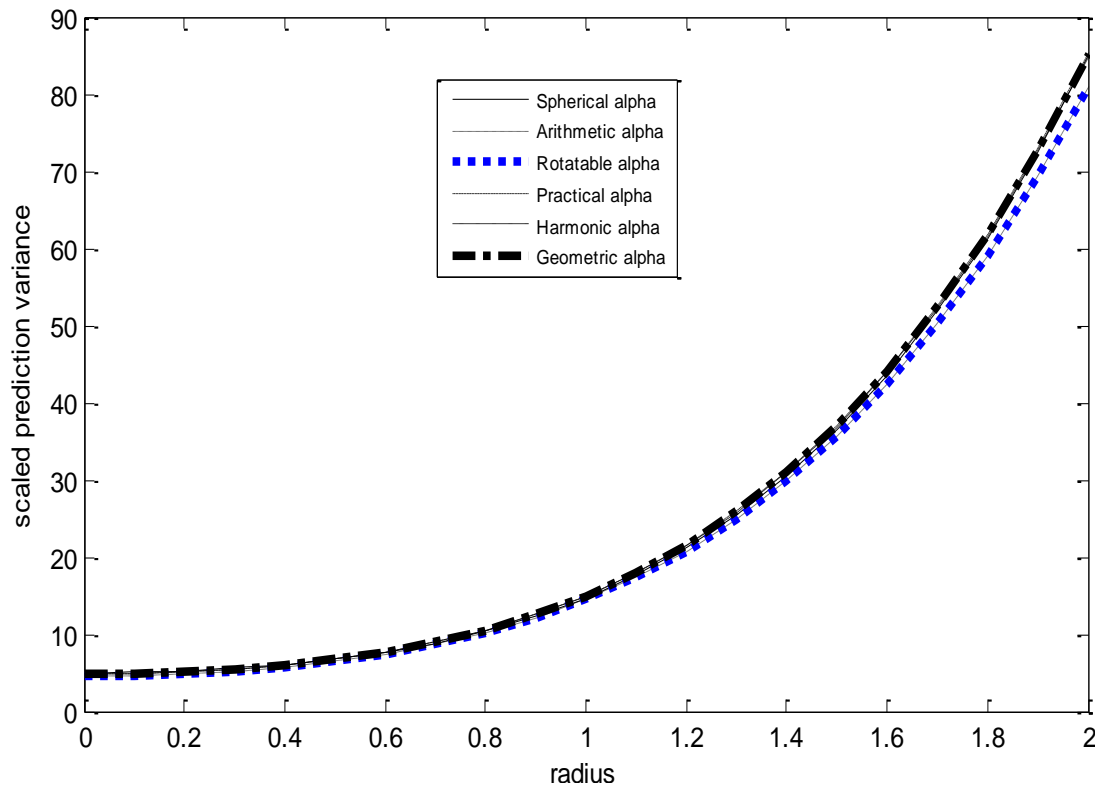


**FIG. 1:** VDG for Two-Factor Star-Replicated CCD with  $n_2 = 2$  in Spherical Region

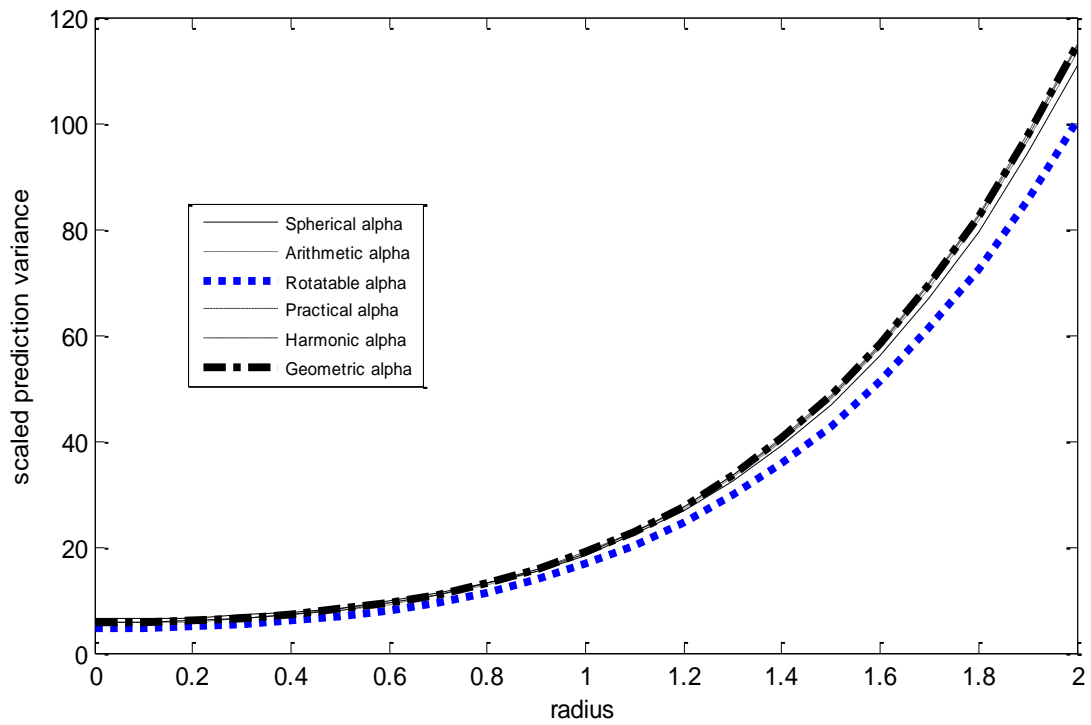


**FIG. 2:** VDG for Two-Factor Star-Replicated CCD with  $n_2 = 3$  in Spherical Region

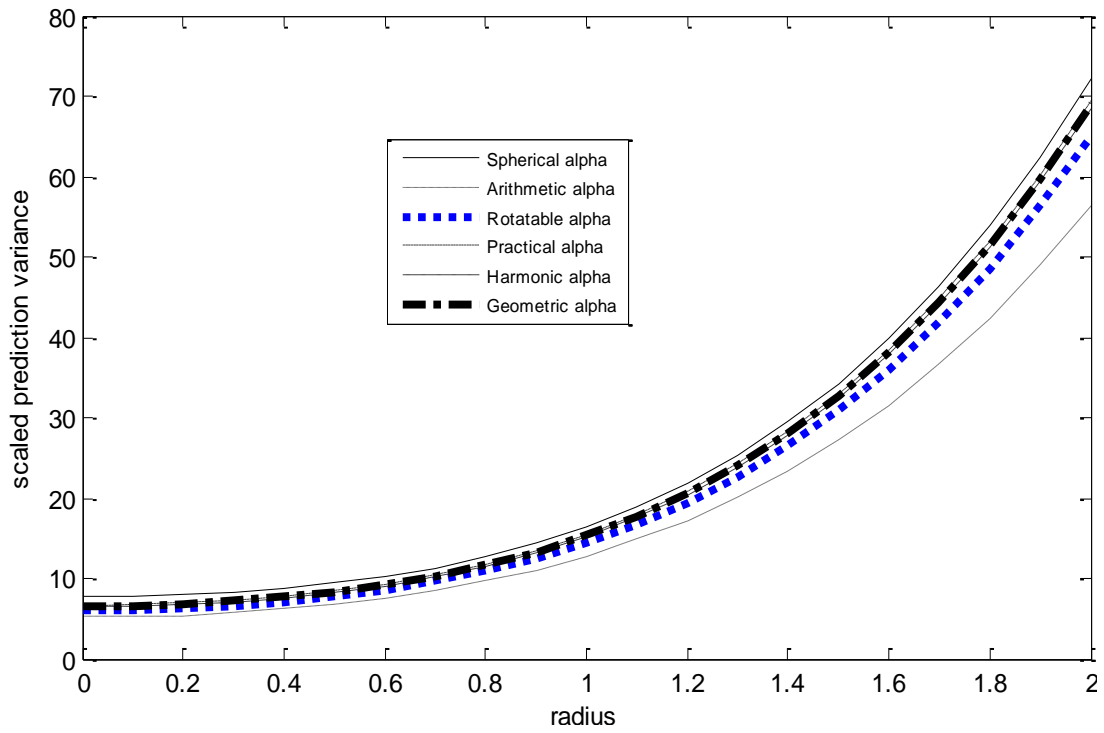


**FIG. 3:** VDG for Three-Factor Star-Replicated CCD with  $n_2 = 2$  in Spherical Region

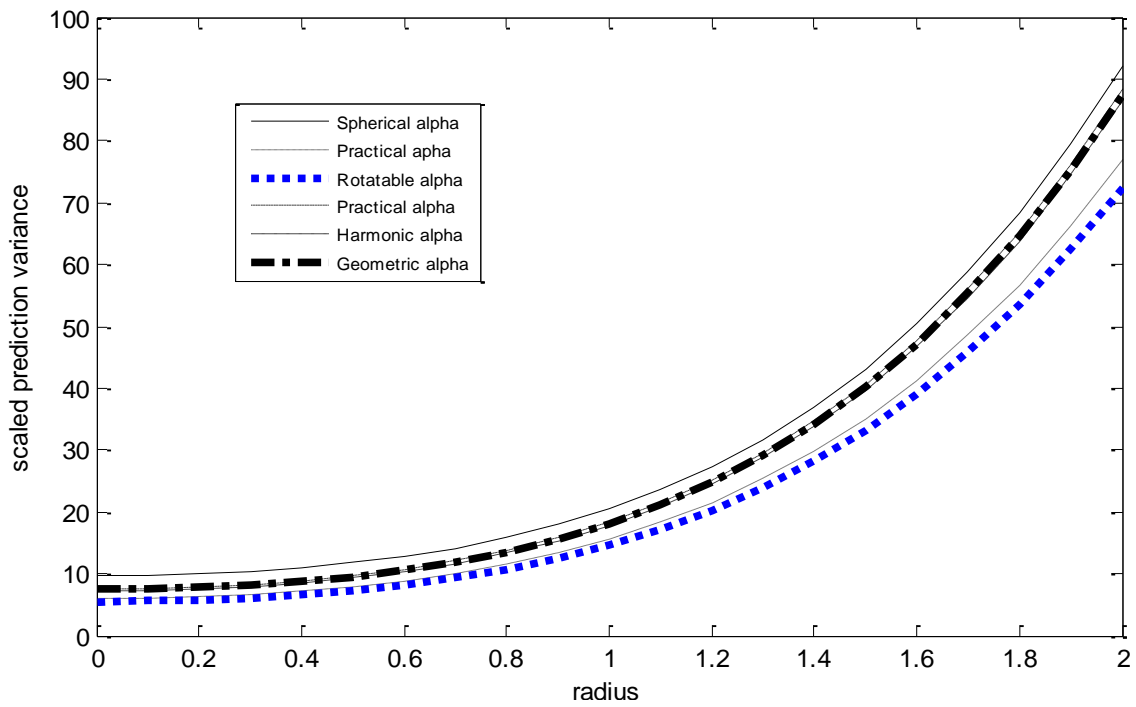


**FIG. 4:** VDG for Three-Factor Star-Replicated CCD with  $n_2 = 3$  in Spherical Region

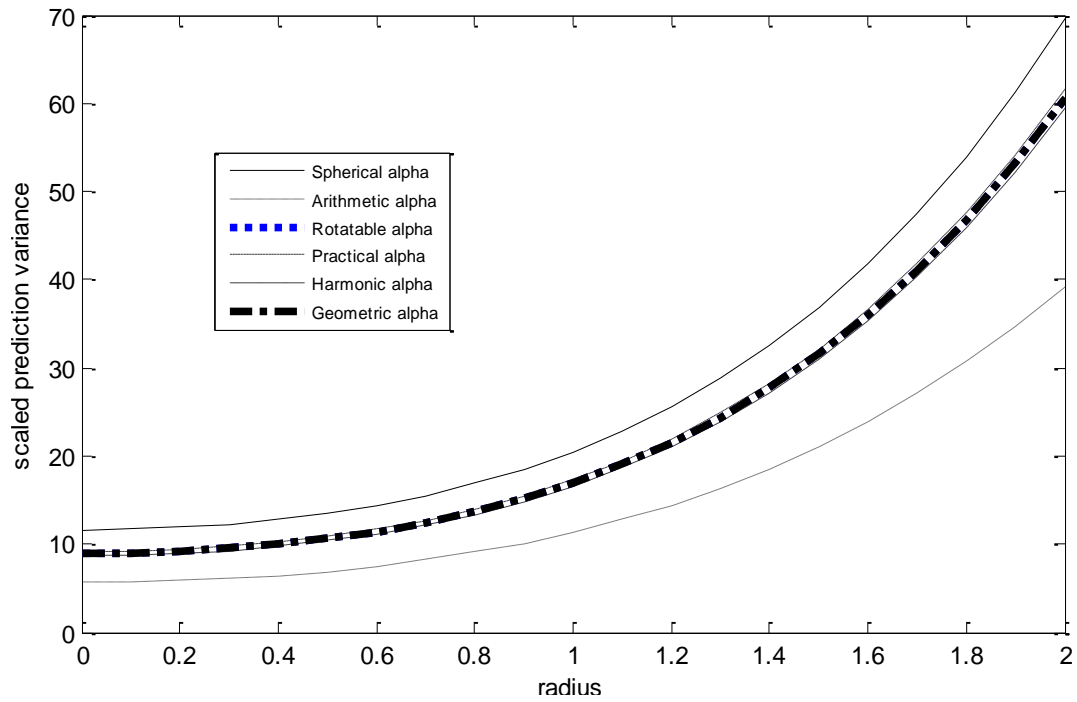


**FIG. 5:** VDG for Four-Factor Star-Replicated CCD with  $n_2 = 2$  in Spherical Region

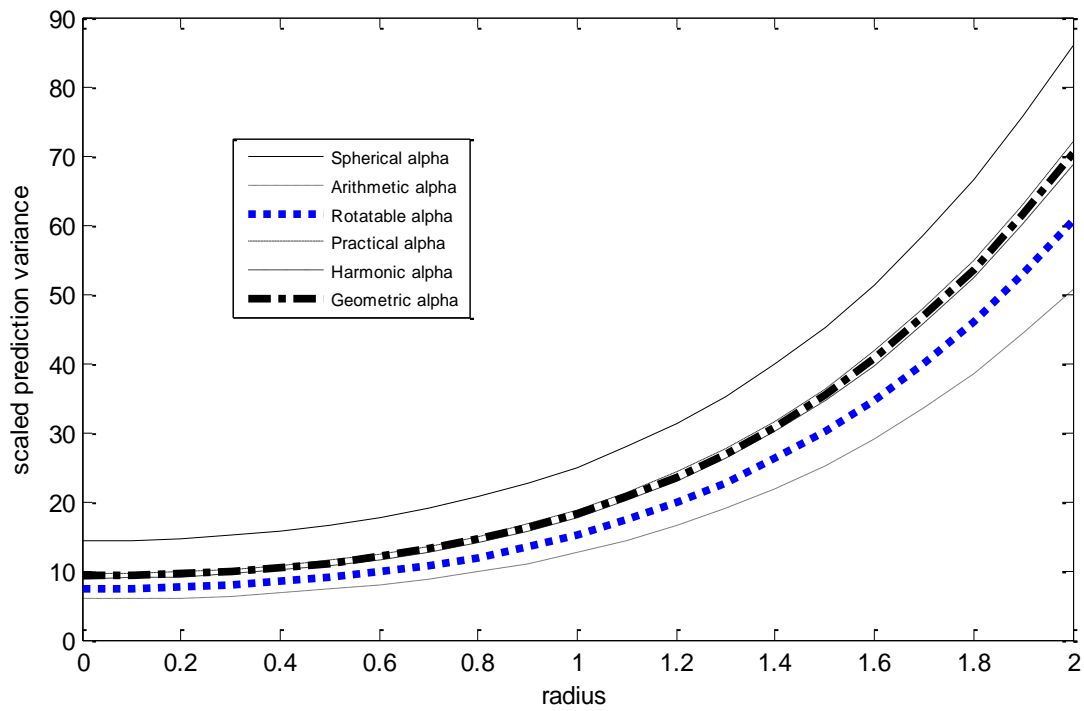


**FIG. 6:** VDG for Four-Factor Star-Replicated CCD with  $n_2 = 3$  in Spherical Region

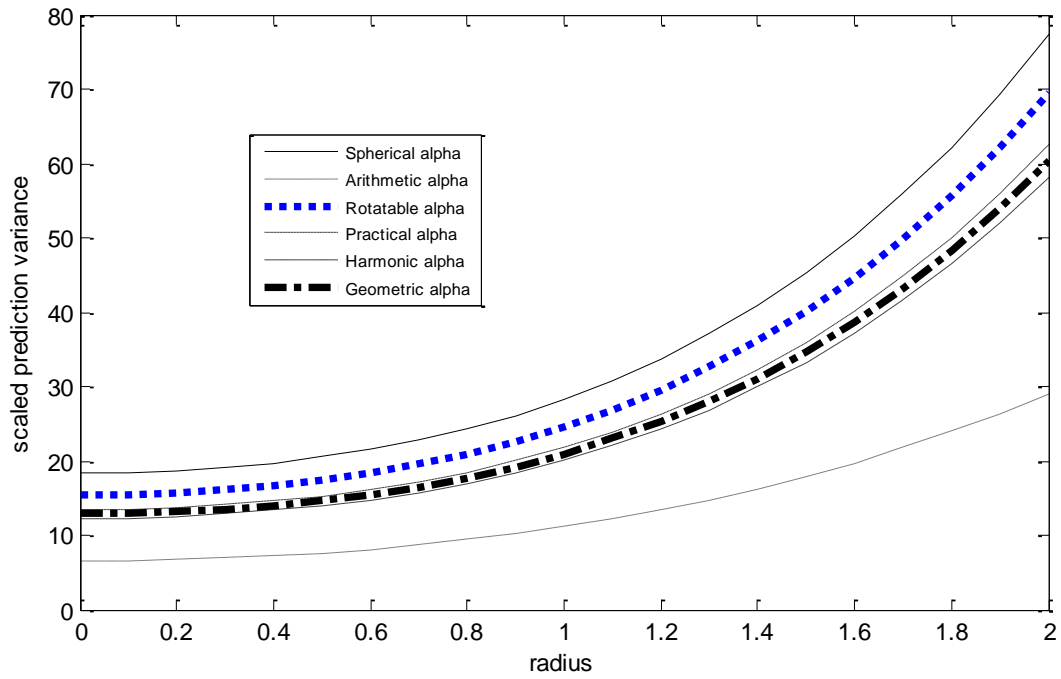


**FIG. 7:** VDG for Five-FactorStar-Replicated CCD with  $n_2 = 2$  in Spherical Region

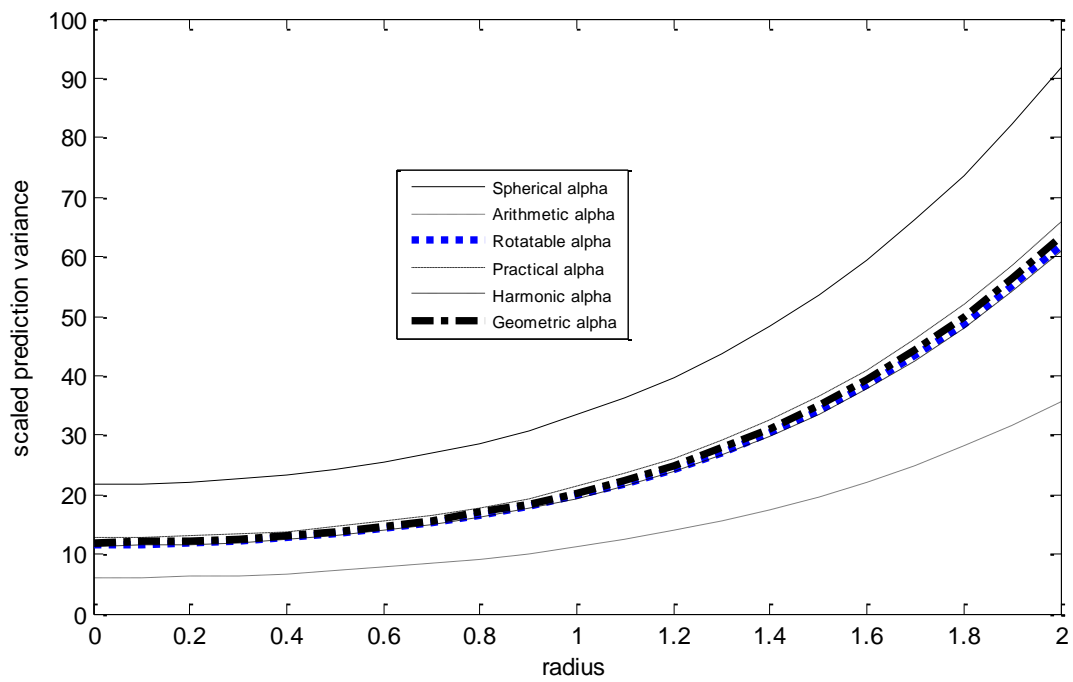


**FIG. 8:** VDG for Five-FactorStar-Replicated CCD with  $n_2 = 3$  in Spherical Region

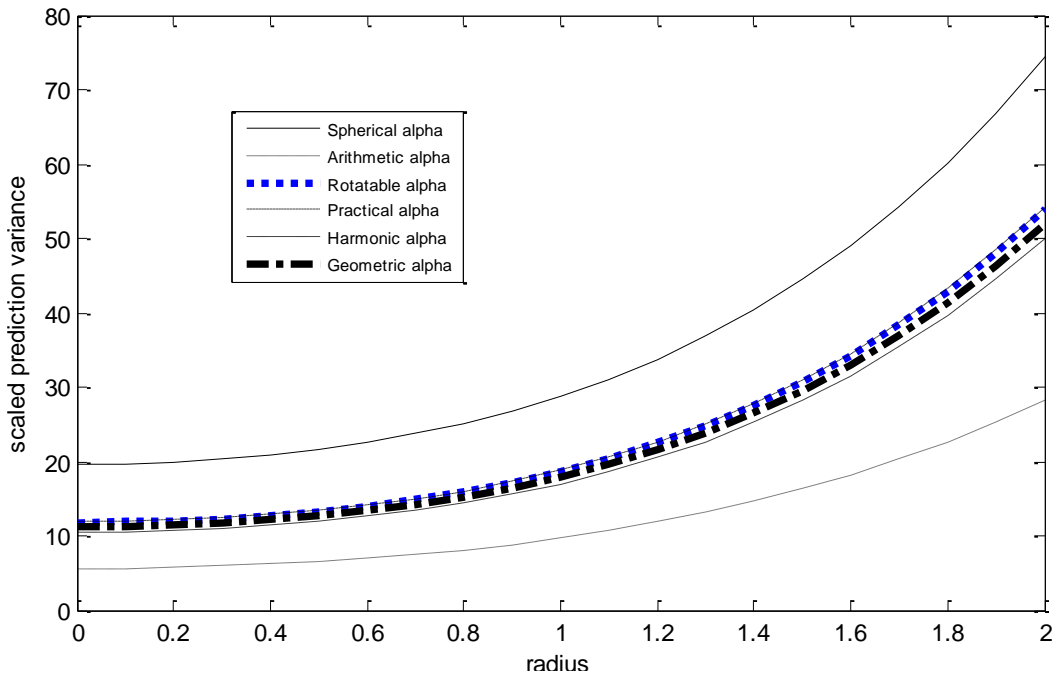


**FIG. 9:** VDG for Six-FactorStar-Replicated CCD with  $n_2 = 2$  in Spherical Region

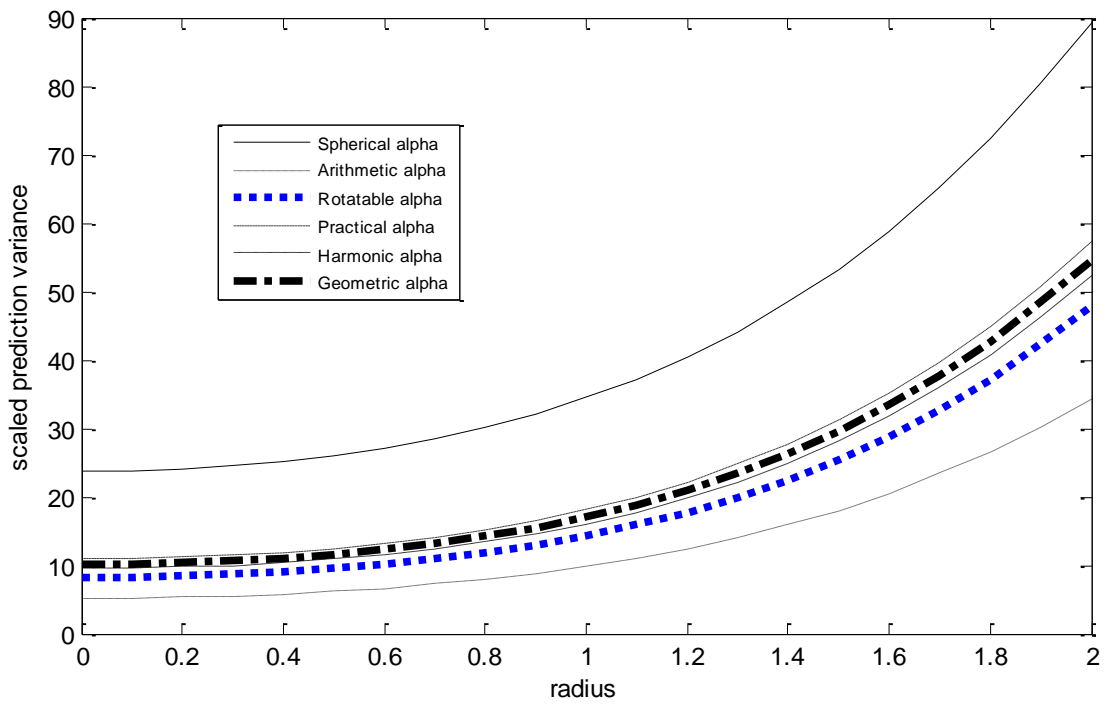


**FIG. 10:** VDG for Six-FactorStar-Replicated CCD with  $n_2 = 3$  in Spherical Region

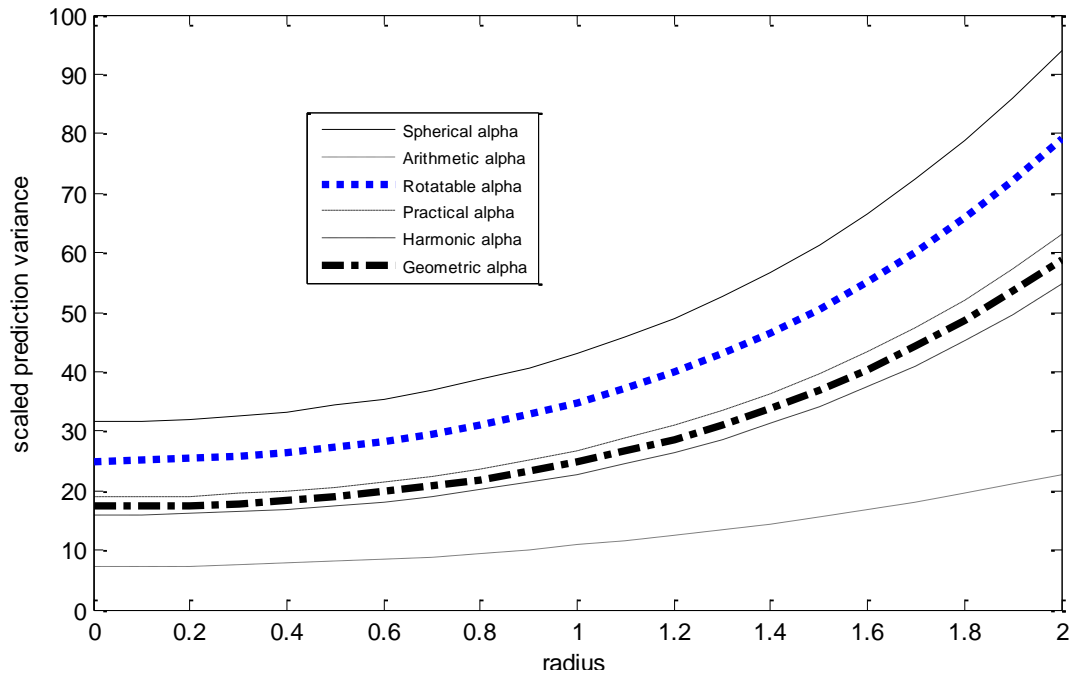


**FIG. 11:** VDG for Seven-Factor Star-Replicated CCD with  $n_2 = 2$  in Spherical Region

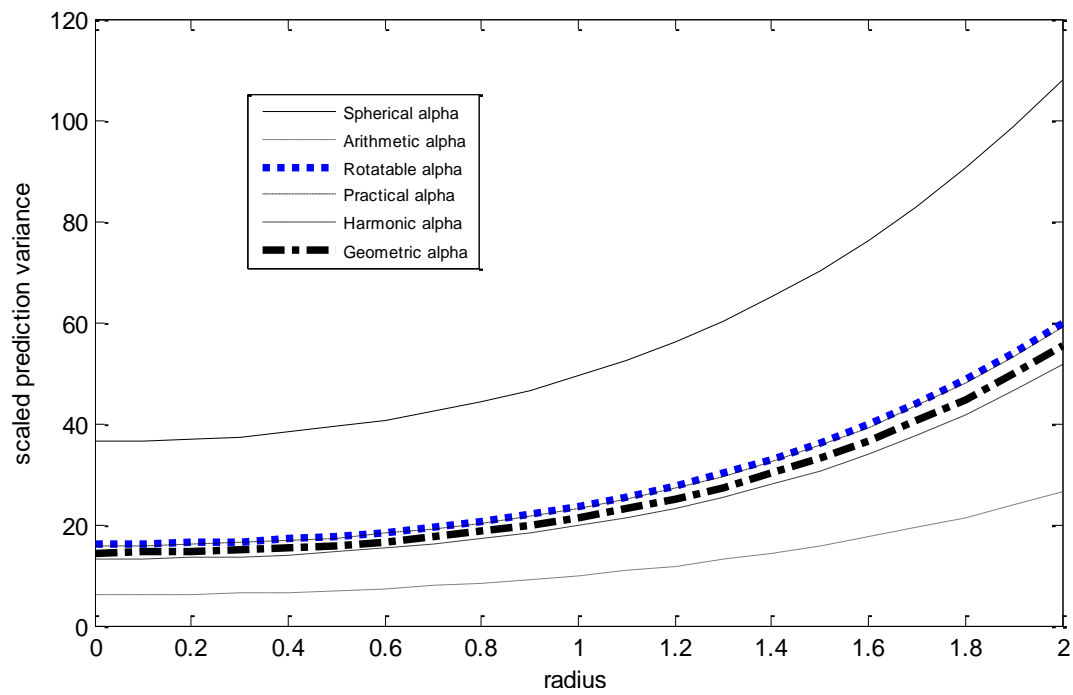


**FIG. 12:** VDG for Seven-Factor Star-Replicated CCD with  $n_2 = 3$  in Spherical Region

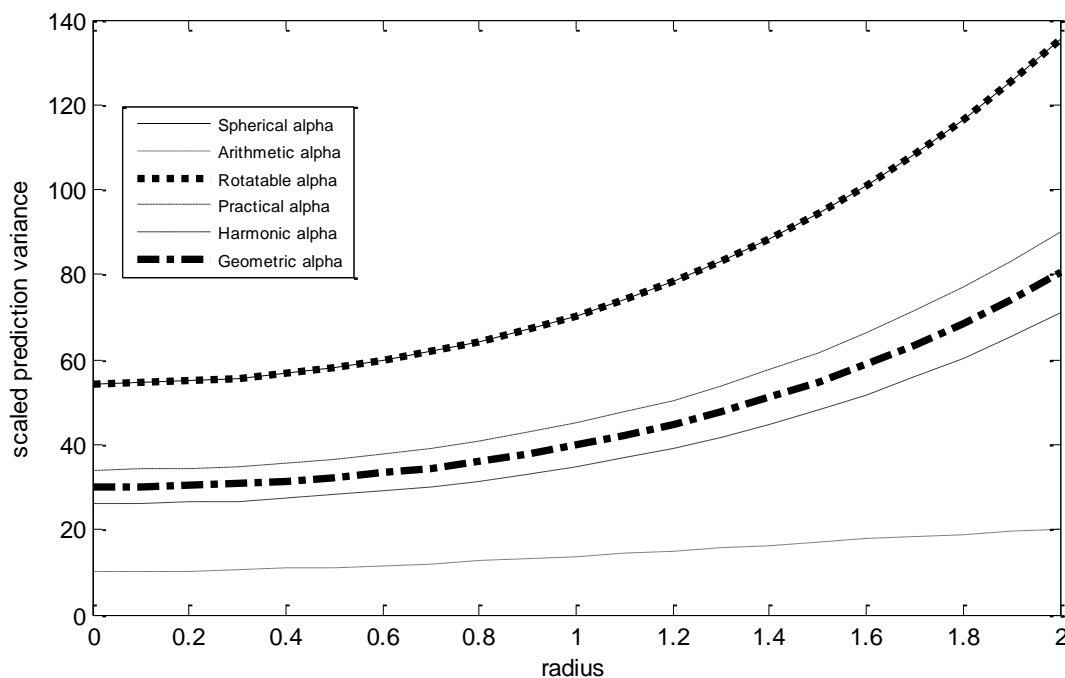


**FIG. 13:** VDG for Eight-Factor Star-Replicated CCD with  $n_2 = 2$  in Spherical Region

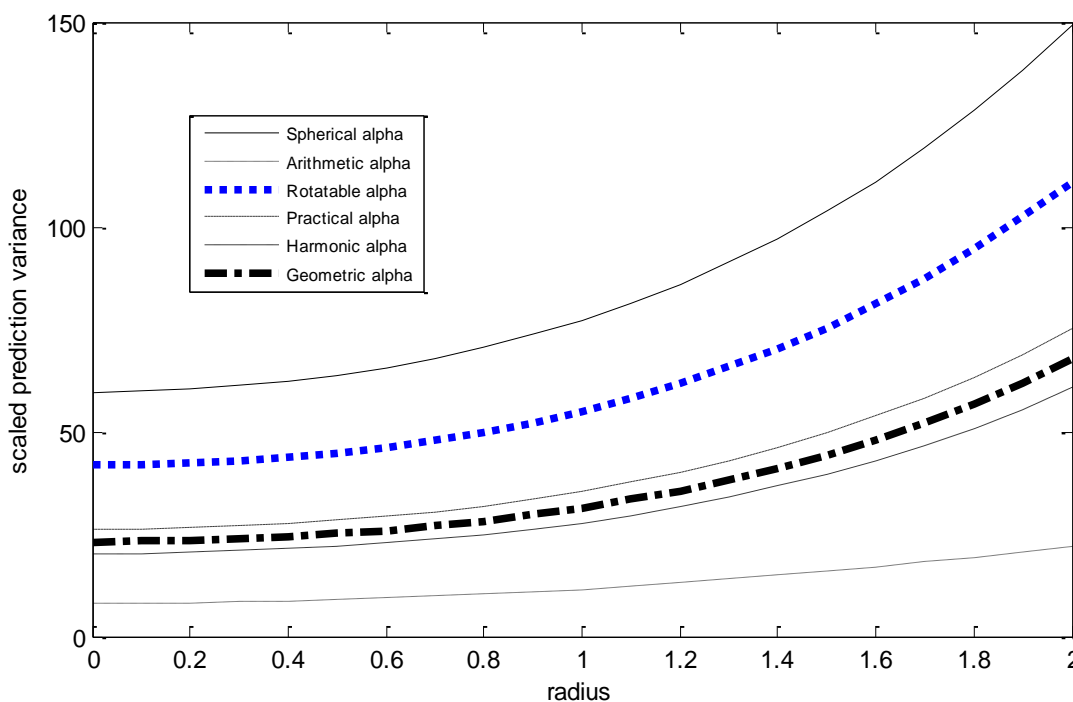


**FIG. 14:** VDG for Eight-Factor Star-Replicated CCD with  $n_2 = 3$  in Spherical Region

The variance dispersion graphs (VDG) for the star-replicated central composite designs are shown in Figures 1 to 14 for  $n_2 = 2$  and 3. For  $k = 2$  factors, all the six competing designs display very similar scaled prediction variance characteristics with almost equal scaled prediction variances and could be described to have equal prediction capabilities, especially for  $n_2 = 2$ . For  $n_2 = 3$ , the CCD with rotatable axial distance gives the lowest scaled prediction variance which is slightly different from the others. The CCD with arithmetic axial distance displayed the lowest and most stable scaled prediction variances for  $k = 3$  to 8 factors and mostly for the  $n_2 = 2$  and 3 replications of the star portion. This is followed by the CCD with harmonic axial distance for some factors and the CCD with rotatable axial distance for other factors. The CCD with spherical axial distance

displayed the worst scaled prediction variance distribution with the highest scaled prediction variance values for all the factors and for  $n_2 = 2$  and 3 replications of the star portion. This is followed by the CCD with practical axial distance.

Should the experimenter decide to harness the advantages of replicating the star portion of the CCD in predicting responses in the spherical region, the CCD with arithmetic axial distance should be the ideal choice. The fact that these competing designs have equal number of experimental runs and centre points shows that the best design in terms of small and stable scaled prediction variance has no undue advantage over the other designs.

Figures 15- 28 are the fraction of design space graphs (FDSG)

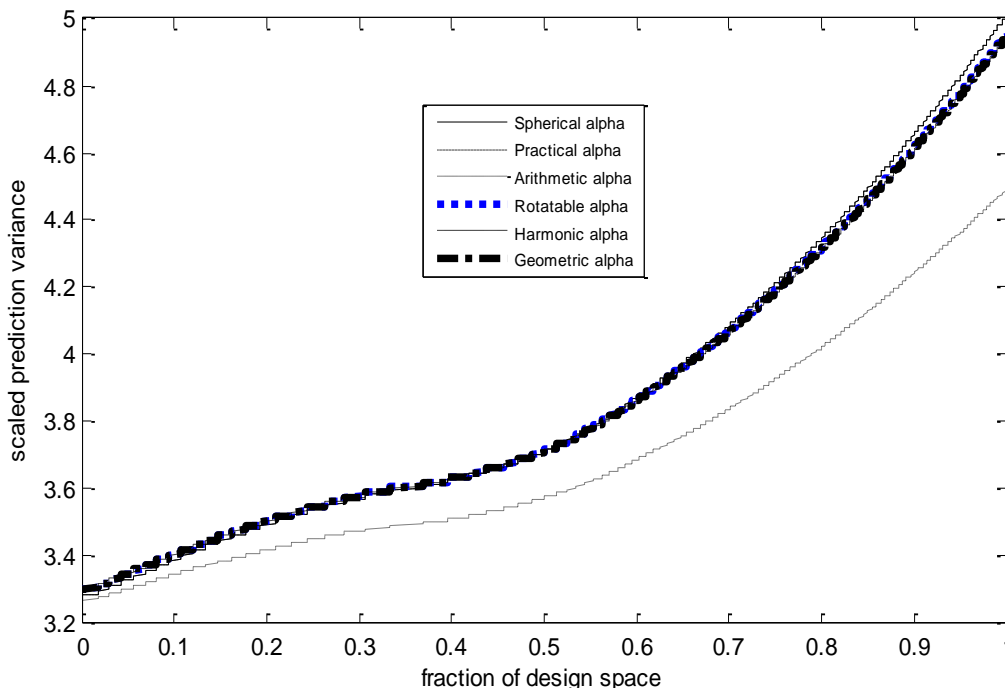
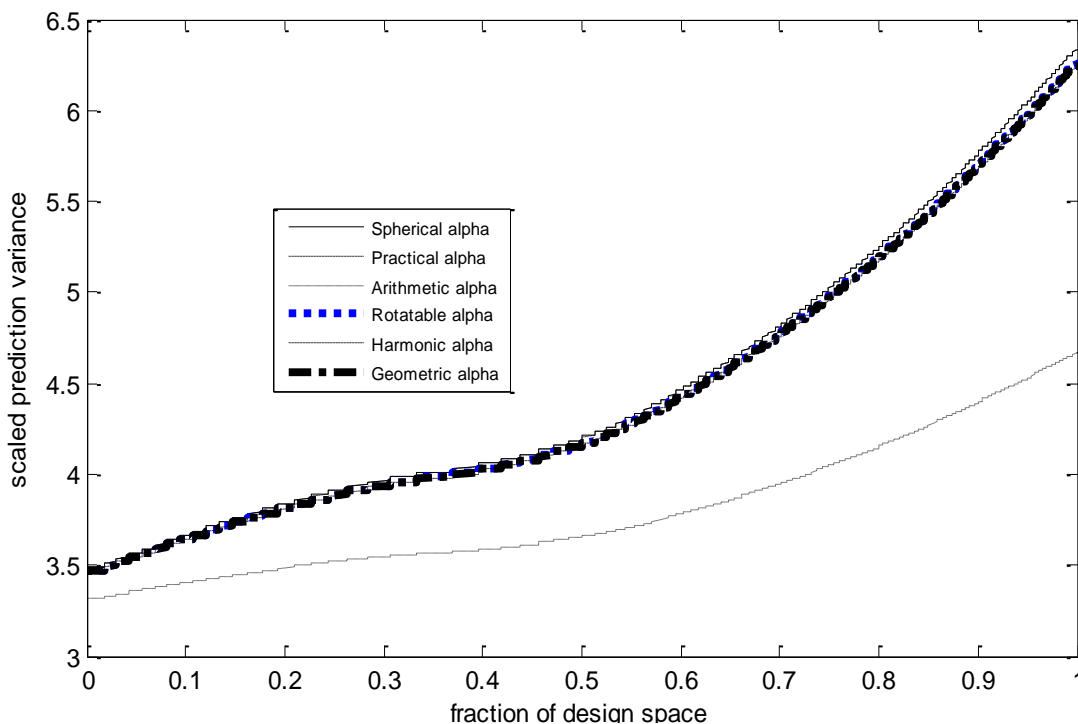
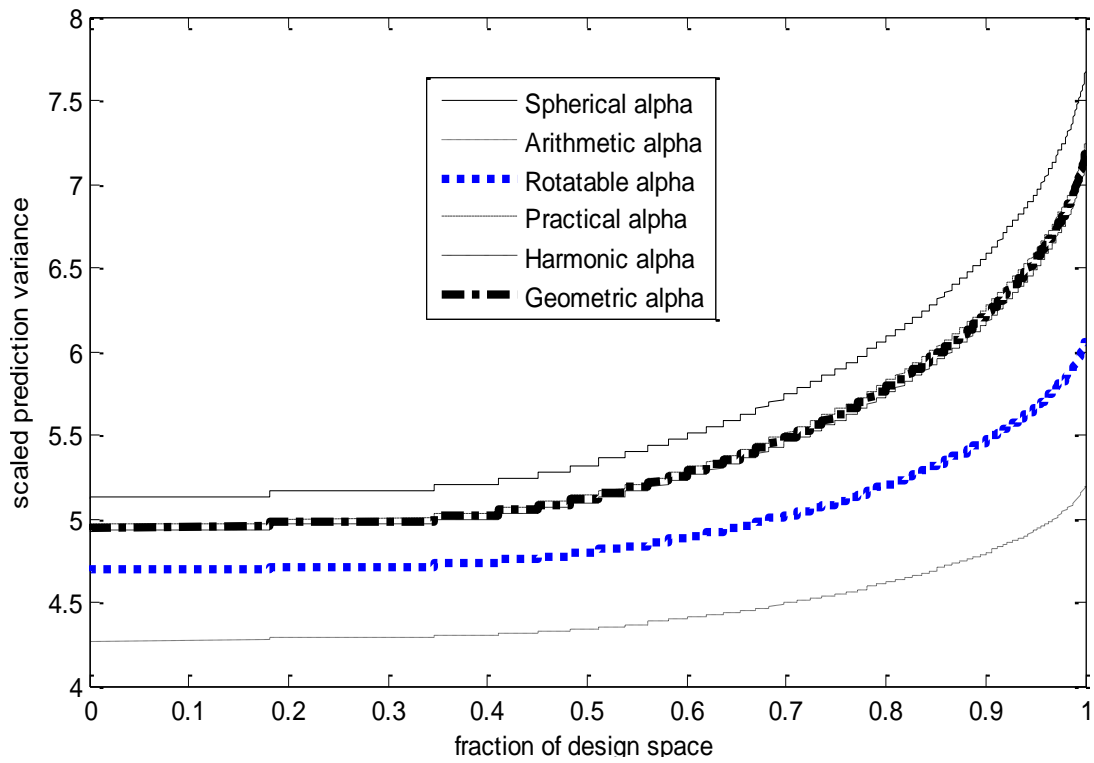


FIG. 15: FDSG for Two-Factor Star-Replicated CCD with  $n_2 = 2$  in Spherical Region



**FIG. 16:** FDSG for Two-Factor Star-Replicated CCD with  $n_2 = 3$  in Spherical Region



**FIG. 17:** FDSG for Three-Factor Star-Replicated CCD with  $n_2 = 2$  in Spherical Region

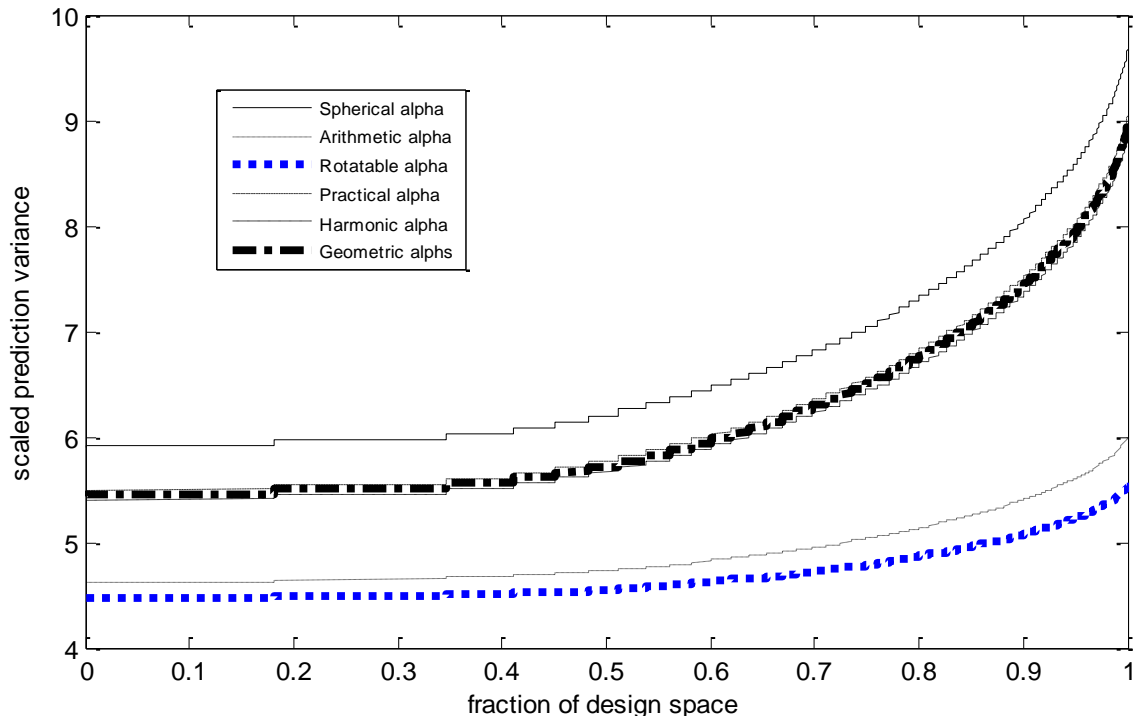


**FIG. 18:** FDSG for Three-Factor Star-Replicated CCD with  $n_2 = 3$  in Spherical Region

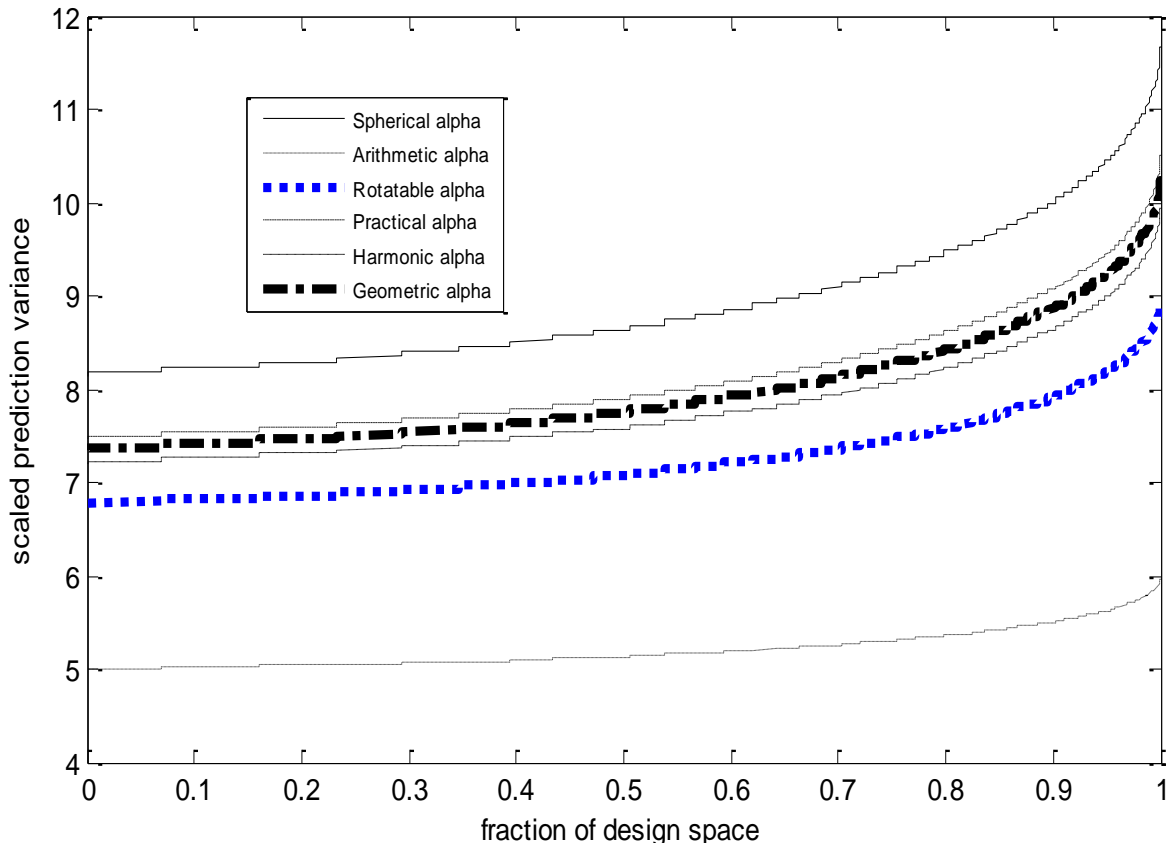


**FIG. 19:** FDSG for Four-Factor Star-Replicated CCD with  $n_2 = 2$  in Spherical Region

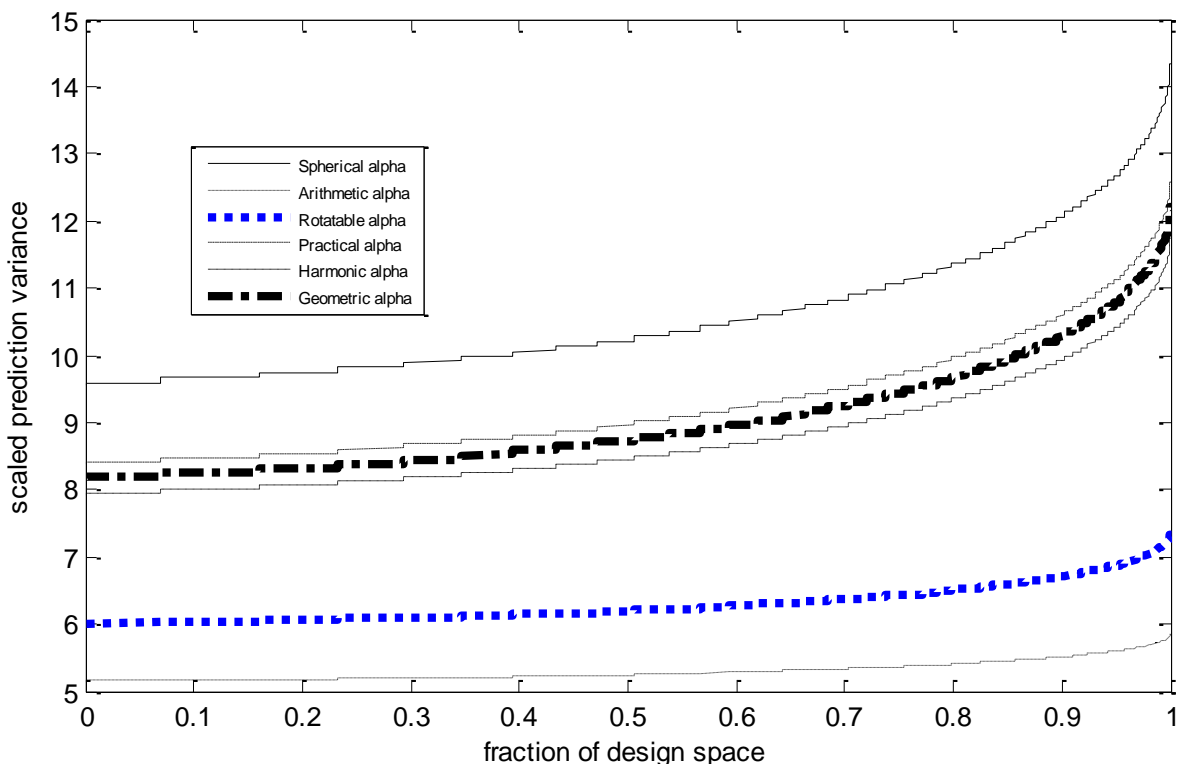


**FIG. 20:** FDSG for Four-Factor Star-Replicated CCD with  $n_2 = 3$  in Spherical Region

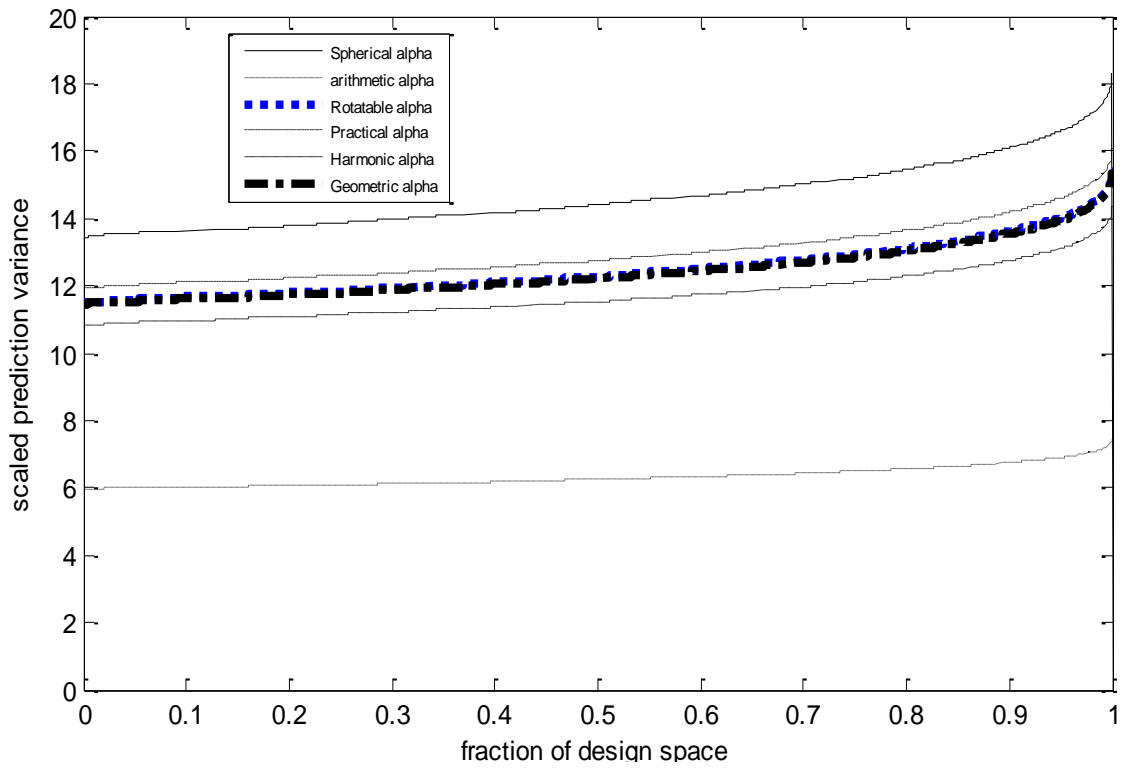


**FIG. 21:** FDSG for Five-Factor Star-Replicated CCD with  $n_2 = 2$  in Spherical Region

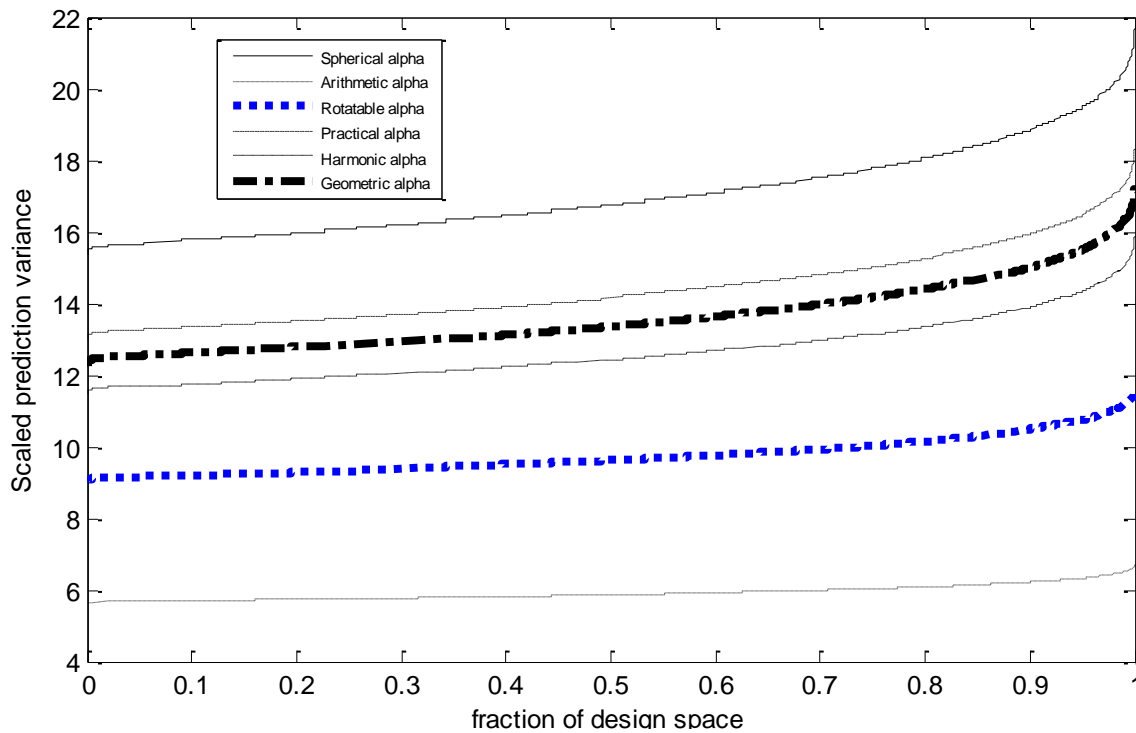


**FIG. 22:** FDSG for Five-Factor Star-Replicated CCD with  $n_2 = 3$  in Spherical Region

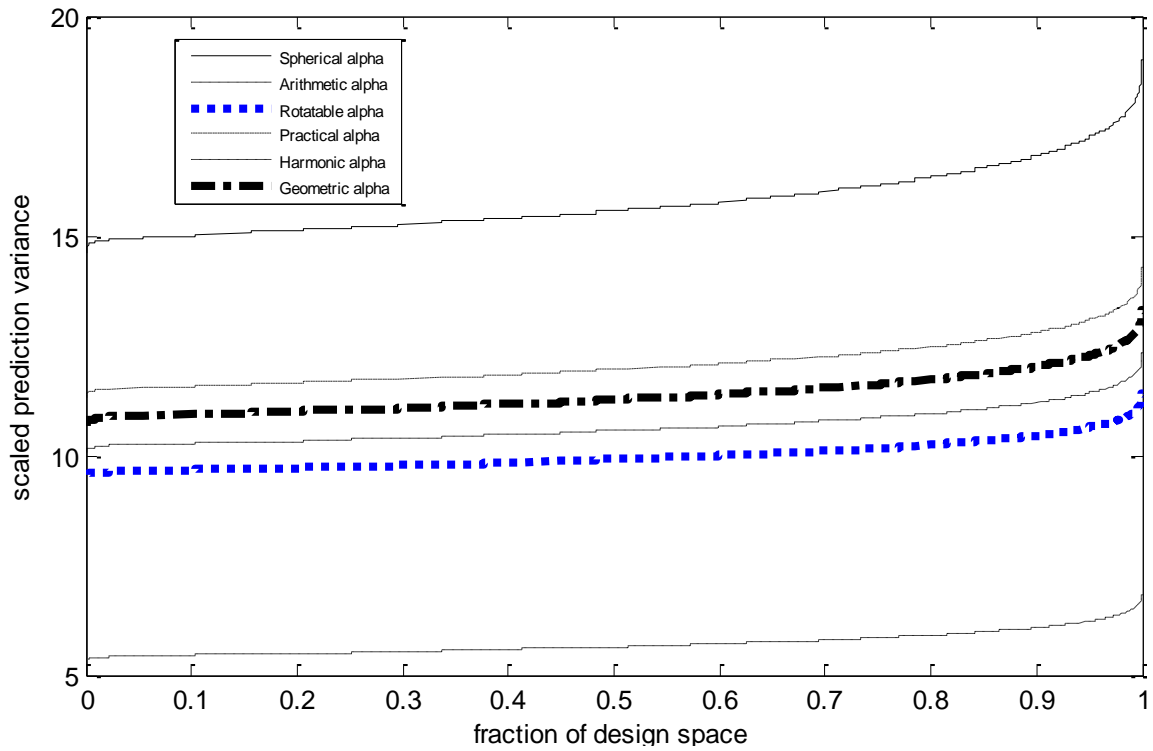


**FIG. 23:** FDSG for Six-Factor Star-Replicated CCD with  $n_2 = 2$  in Spherical Region

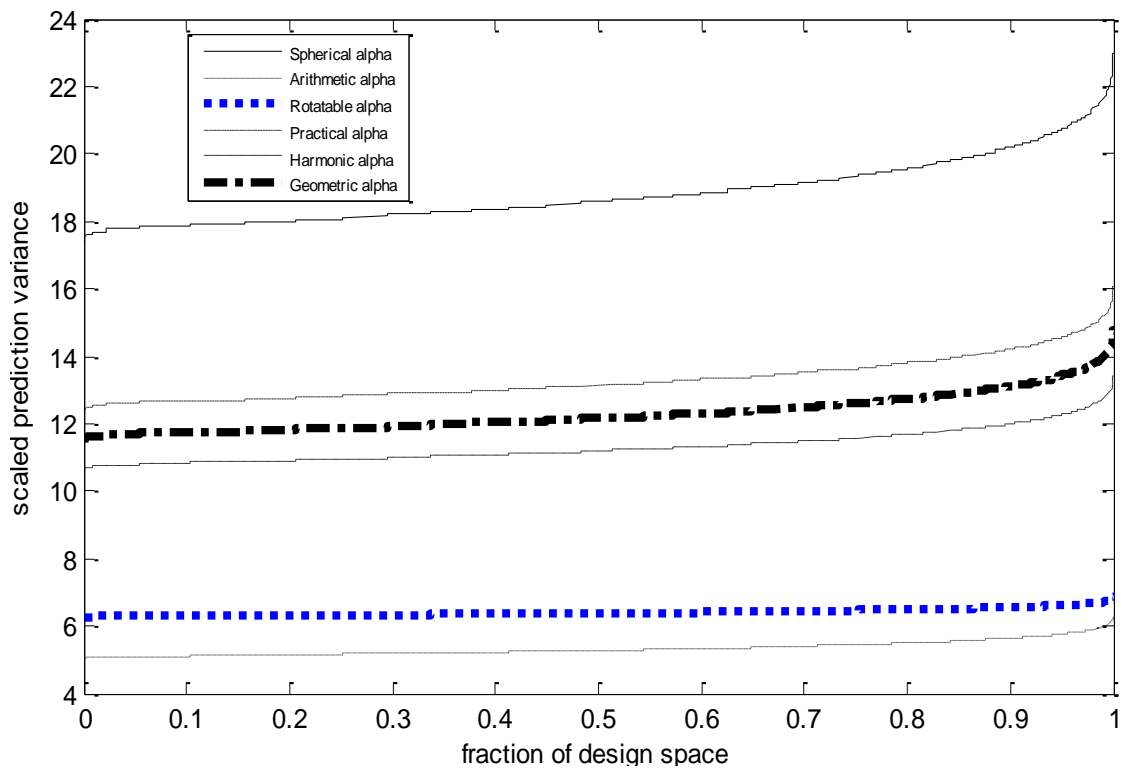


**FIG. 24:** FDSG for Six-Factor Star-Replicated CCD with  $n_2 = 3$  in Spherical Region

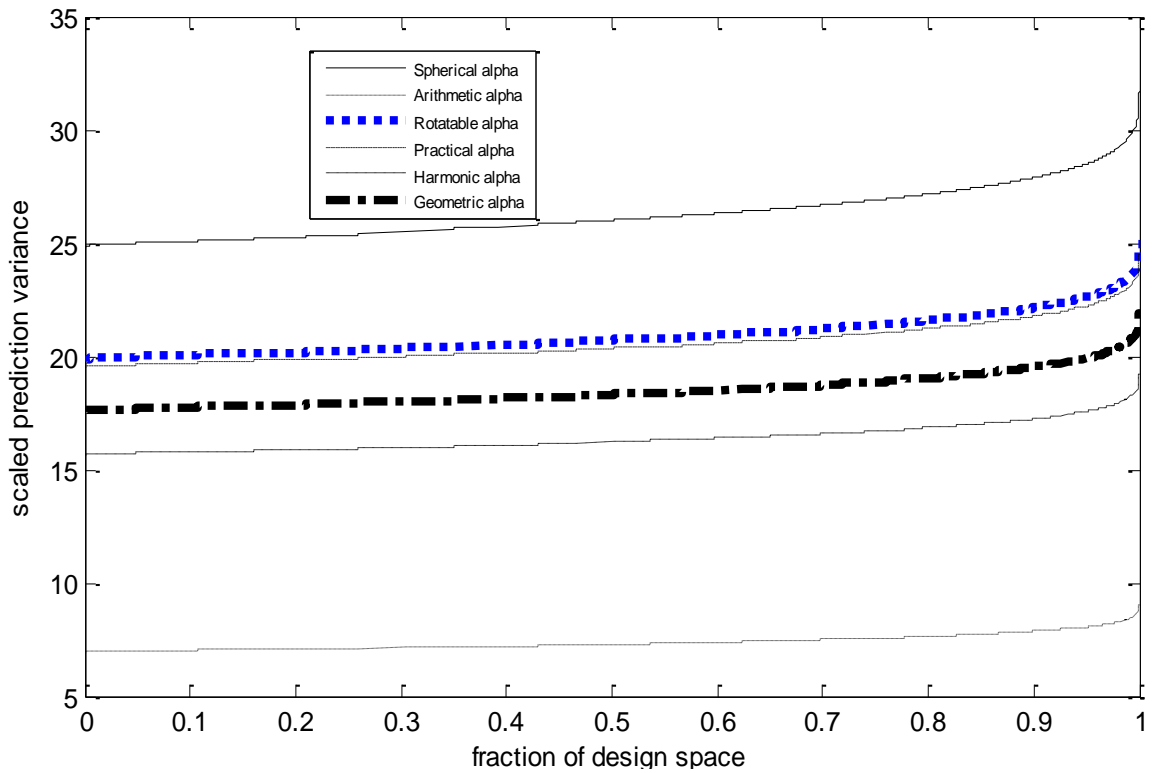


**FIG. 25:** FDSG for Seven-Factor Star-Replicated CCD with  $n_2 = 2$  in Spherical Region

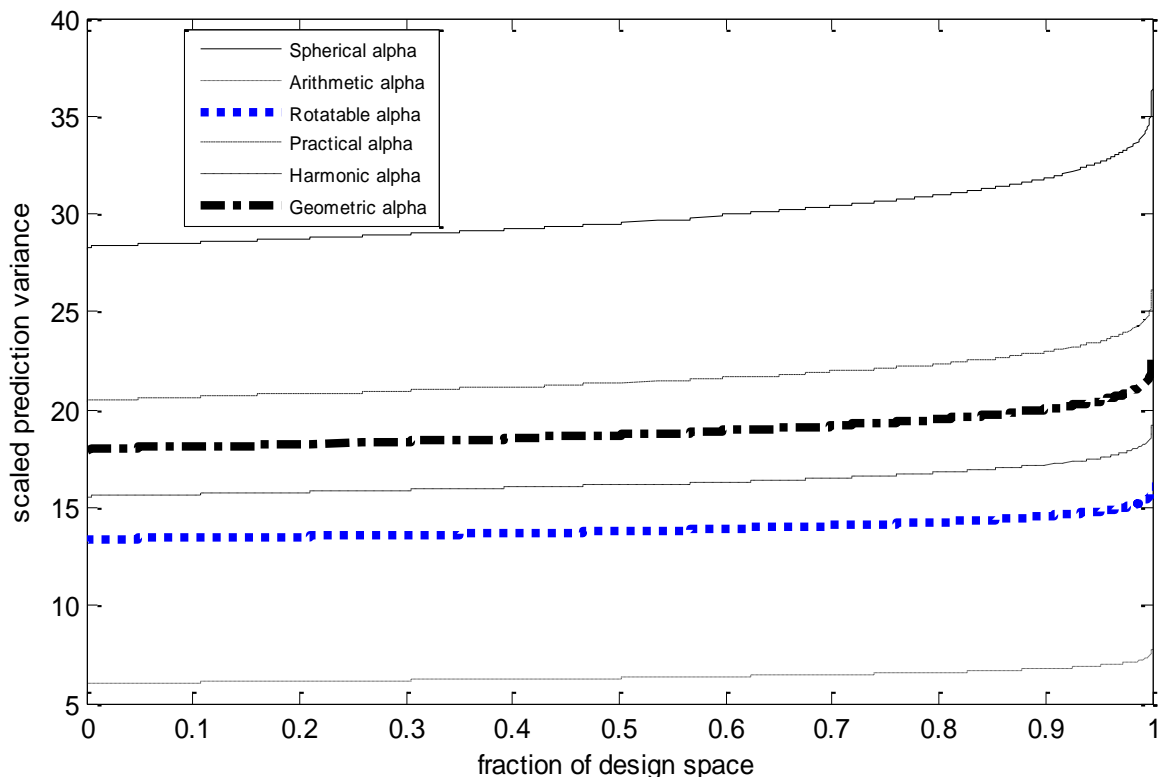


**FIG. 26:** FDSG for Seven-Factor Star-Replicated CCD with  $n_2 = 3$  in Spherical Region

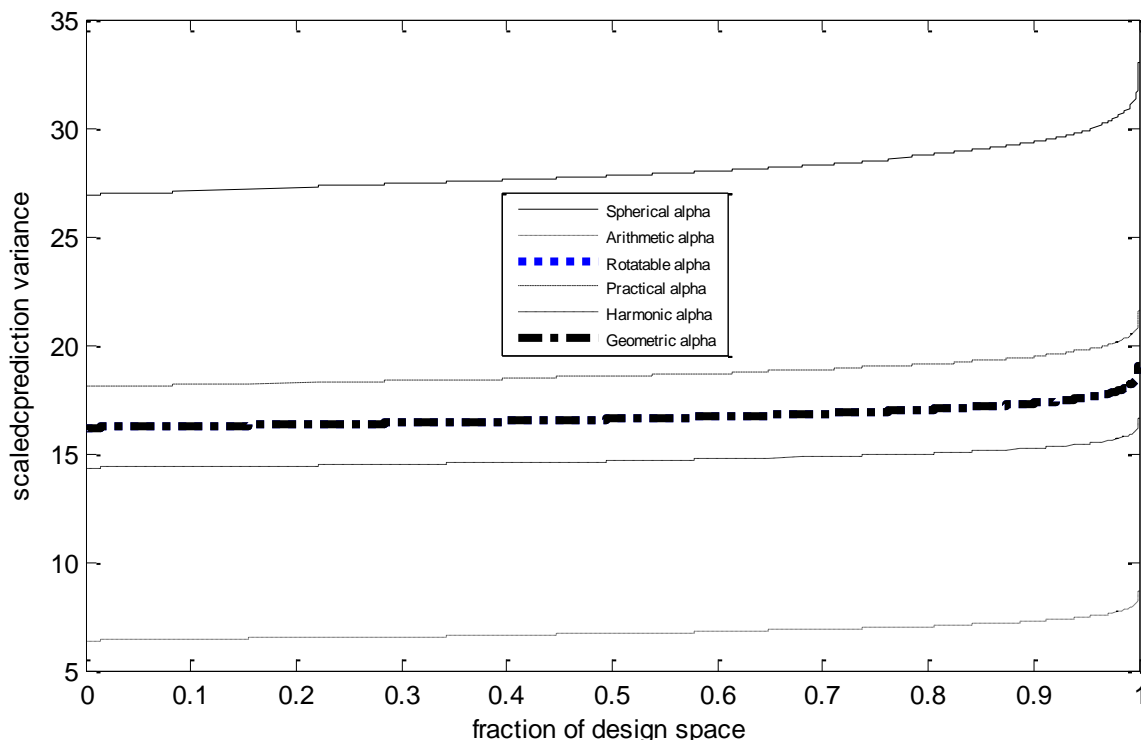


**FIG. 27:** FDSG for Eight-Factor Star-Replicated CCD with  $n_2 = 2$  in Spherical Region

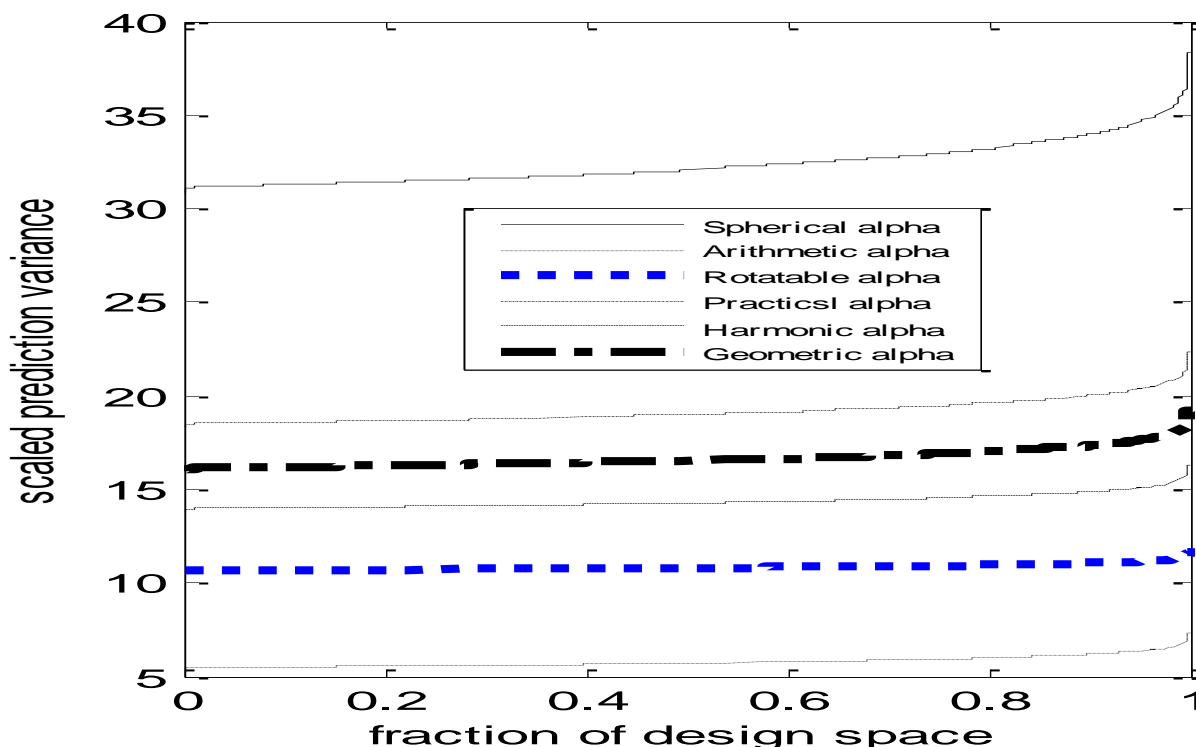


**FIG. 28:** FDSG for Eight-Factor Star-Replicated CCD with  $n_2 = 3$  in Spherical Region

The fraction of design space graphs of Figures 15 to 28 show that the CCD with arithmetic axial distance gives the smallest scaled prediction variances throughout the spherical region for  $n_2 = 2$  and 3 replications of the star portion and for the  $k = 2, 3, \dots, 8$  experimental factors under consideration. The CCD with harmonic alpha is the second best for all the factors only when there is  $n_2 = 2$  replication of the star portion. The scaled prediction variances of the CCD with rotatable axial distance get smaller and better as the replication of the star portion increases from  $n_2 = 2$  to  $n_2 = 3$  and performed better than the CCD with arithmetic alpha for  $k = 3$



with  $n_2 = 3$ . The CCD with spherical axial distance gives the worst prediction variance performances with the highest and most unstable scaled prediction variances for  $n_2 = 2$  and 3 and for all the factors under consideration. This is followed by the CCD with practical axial distance which displayed the second worst scaled prediction variance characteristics throughout the entire design space. The graphs did not reflect any improvement in the prediction capabilities of the CCDs with spherical and practical axial distances with the replication of the star portion.

#### 4 Conclusion

In conclusion, the replication of the star portion of the CCD improved the prediction variance characteristics of the variations of the CCD in the spherical regions. However, the variation of the CCD with arithmetic axial distance is the smallest and most stable scaled prediction variance characteristics in the spherical region as displayed in the VDG and FDSG.

#### References

1. Borkowski, J. J. (1995). Spherical Prediction Properties of Central Composite and Box Behnken Designs, *Technometrics*, Vol. 37 (4), 399 - 410. <https://doi.org/10.1080/00401706.1995.10484373>
2. Chigbu, P. E., Ukaegbu, E. C. & Nwanya, J. C. (2009). On Comparing the Prediction Variances of Some Central Composite Designs in Spherical Region: A Review, *Statistica*, anno LXIX, n.4, 285-298.
3. Chigbu, P. E. & Ohaegbulem, U. O. (2011). On the Preference of Replicating Factorial Runs to Axial Runs in Restricted Second-Order Designs, *Journal of Applied Sciences*, Vol. 11 (22), 3732 - 3737. <https://doi.org/10.3923/jas.2011.3732.3737>
4. Draper, N. R. (1982). Centre Points in Second-Order Response Surface Designs, *Technometrics*, Vol. 24 (2), 127 - 133. <https://doi.org/10.1080/00401706.1982.10487734>
5. Dykstra, O. Jr. (1959). Partial Duplication of Factorial Experiments, *Technometrics*, Vol. 1 (1), 63 - 75. <https://doi.org/10.1080/00401706.1959.10489849>
6. Dykstra, O. Jr. (1960). Partial Duplication of Response Surface Designs, *Technometrics*, Vol. 2 (2), 185 - 195. <https://doi.org/10.1080/00401706.1960.10489893>
7. Giovannitti-Jensen, A. & Myers, R.H. (1989). Graphical Assessment of the Prediction Capability of Response Surface Designs, *Technometrics*, Vol. 31 (2), 159 - 171. <https://doi.org/10.1080/00401706.1989.10488510>
8. Li, J., Liang, L., Borror, C. M., Anderson-Cook, C. M. & Montgomery, D.C. (2009). Graphical Summaries to Compare Prediction Variance Performance for Variations of the Central Composite Design for 6 to 10 Factors, *Quality Technology and Quantitative Management*, Vol. 6 (4), 433 - 449. <https://doi.org/10.1080/16843703.2009.11673209>
9. Onyishi, L.I and Eze, F.C. (2020). Alternative Axial Distances for Spherical Regions of Central Composite Designs. *Earthline Journal of Mathematical Sciences* Volume 4, Number 2, pp 273-285. <https://doi.org/10.34198/ejms.4220.273285>
10. Onukogu, I. B. (1997). *Foundations of Optimum Exploration of Response Surfaces*, Ephrata Press, Nsukka.
11. Ozol-Godfrey, A., Anderson-Cook, C. M. & Montgomery, D. C. (2005). Fraction of Design Space Plots for Examining Model Robustness, *Journal of Quality Technology*, Vol. 37, 223 - 235. <https://doi.org/10.1080/00224065.2005.11980323>
12. Ukaegbu, E. C. (2017). *Evaluation of Prediction Capabilities of Partially Replicated Variations of Some Central Composite Design*, A PhD Thesis Submitted to the Department of Statistics, University of Nigeria, Nsukka.
13. Ukaegbu, E. C. & Chigbu, P. E. (2015a). Characterization of Prediction Variance Properties of Rotatable Central Composite Designs for 3 to 10 Factors, *International Journal of Computational & Theoretical Statistics*, Vol. 2 (2), pp. 87 - 97. <https://doi.org/10.12785/ijcts/020203>

14. [Ukaegbu, E. C. & Chigbu, P. E. (2015b). Graphical Evaluation of the Prediction Capabilities of Partially Replicated Orthogonal Central Composite Designs, *Quality and Reliability Engineering International*, Vol. 31, pp. 707 - 717, DOI: 10.1002/qre.1630. <https://doi.org/10.1002/qre.1630>